

Investigation of the pin-roller metering device and tube effect for wheat seeds and granular fertilizers based on DEM

Sugirbay Adilet^{1,2,3}, Kaiyuan Zhao¹, Guangyao Liu¹, Nukeshev Sayakhat³, Jun Chen^{1*},
Guangrui Hu¹, Lingxin Bu⁴, Yu Chen¹, Hongling Jin¹, Shuo Zhang¹,
Zagainov Nikolay^{1,3}, Muratkhan Marat³

- (1. College of Mechanical and Electronic Engineering, Northwest A&F University, Xianyang 712100, Shaanxi, China;
2. College of Water Resources and Architectural Engineering, Northwest A&F University, Xianyang 712100, Shaanxi, China;
3. Technical Faculty, S. Seifullin Kazakh Agrotechnical University, Astana 010000, Kazakhstan;
4. College of Mechatronic Engineering, North Minzu University, Yinchuan 750021, China)

Abstract: The metering device is the central part of the seeder discharging granular fertilizers or seeds from the hopper to the colter passing through the tube. Depending on the metering device design, the batches of particles are discharged or discharged evenly. This research analyzes existing metering devices, and a new pin-roller metering device is recommended to discharge evenly high doses of granular fertilizers and wheat seeds at low rotation speeds. The objective was to adapt the metering device to precision agriculture so that a little electric motor containing gearbox drives every metering device. Therefore, the pin-roller metering device parameters were investigated to apply high doses of granular fertilizers and wheat seeds evenly. The optimal pin positions were determined according to response surface methods (RSM) by simulating the granular fertilizers and wheat seeds' behavior on DEM. The coefficient of variation (CV) and the slip rate (SR) of the particles between the pins were chosen as indicators for evaluating the pin-roller. The shape of the pin was specified, and then the number of lines, the number of pins in a line, and the pin height were chosen to optimize. The analysis of the simulation results shows the optimal parameters: the number of pins in a line is four, and the number of lines is sixteen. The SR of granular fertilizers and wheat seeds were 8% and 2%, respectively. The pin-roller metering device is compared with the six-grooved and twelve-grooved metering devices. The comparison results show that the pin-roller metering device distributes twice more uniformly than other metering devices. The CV of the granular fertilizer distribution for six-grooved, twelve-grooved, and pin-roller metering devices was 111.13%, 80.74%, and 37%, respectively. The CV of the wheat seed distribution for twelve-grooved and pin-roller metering devices was 96%, and 37%, respectively. As long as the particles interact with the tube, leaving the metering device, the effect of tube type and position is investigated. As a result, it was determined that the tube has minimal effect on the pin-roller metering device while positively impacting the six-grooved and twelve-grooved metering devices, improving the CV of the particle distribution into the soil.

Keywords: pin-roller, metering device, DEM, coefficient of variation, slippage rate, tube

DOI: [10.25165/ijabe.20231602.7721](https://doi.org/10.25165/ijabe.20231602.7721)

Citation: Adilet S, Zhao K Y, Liu G Y, Sayakhat N, Chen J, Hu G R, et al. Investigation of the pin-roller metering device and tube effect for wheat seeds and granular fertilizers based on DEM. *Int J Agric & Biol Eng*, 2023; 16(2): 103–114.

1 Introduction

The metering devices are a significant part of the seeders delivering the fertilizers or seeds from the hopper to apply into the soil. Nowadays, information technology has reached the level that seeders discharge variable rates of fertilizers or seeds based on a prescription map^[1]. Electric motors drive the metering devices to apply the optimum granular fertilizers or wheat seeds rate in precision farming systems^[2-6]. Moreover, metering devices are

installed on unmanned aerial vehicles driven by electric motors^[7,8]. Given that the development of automatic seeders is a new direction developing a seeder equipped with a small-sized electric motor is of great importance.

The parallel-grooved metering device is one of the most commonly used metering devices for precision farming systems^[9-11]. However, the wheat seeds are distributed unevenly at low rotational speeds of the metering device^[12-15]. The uneven distribution of fertilizers and wheat seeds causes competition between plants and

Received date: 2022-06-06 **Accepted date:** 2023-02-17

Biographies: Sugirbay Adilet, Post-doctoral, research interest: precision agriculture and computer modeling, Email: sugirbayadilet@nwfau.edu.cn; Kaiyuan Zhao, MS candidate, research interest: precision agriculture, Email: Kyz@nwfau.edu.cn; Guangyao Liu, MS candidate, research interest: precision agriculture, Email: xiaoliuganfanren@nwfau.edu.cn; Nukeshev Sayakhat, Professor, research interest: precision agriculture and mathematical modeling, Email: s.nukeshev@kazatu.kz; Guangrui Hu, Phd candidate, research interest: agricultural mechanization and fruit harvesting, Email: 2017050952@nwfau.edu.cn; Lingxin Bu, PhD, research interest: agricultural mechanization and fruit harvesting, Email: 2021023@nmu.edu.cn; Yu Chen, Associate Professor, research interest: agricultural engineering and information technology, Email:

jdx73@nwfau.edu.cn; Hongling Jin, Associate Professor, research interest: agricultural engineering and information technology, Email: jhl@nwsuaf.edu.cn; Shuo Zhang, Associate Professor, research interest: agricultural engineering and information technology, Email: zhangshuo@nwfau.edu.cn; Zagainov Nikolay, PhD candidate, research interest: agricultural engineering and information technology, Email: zagainov@nwfau.edu.cn; Muratkhan Marat, PhD candidate, research interest: agricultural engineering, Email: marat@nwfau.edu.cn.

***Corresponding author:** Jun Chen, Professor, research interest: precision agriculture, agricultural mechanization, and fruit harvesting. College of Mechanical and Electronic Engineering, Northwest A&F University, Xianyang 712100, Shaanxi, China. Tel: +86-13572191773, Email: chenjun_jdx@nwfau.edu.cn.

yield loss^[16-24]. Even distribution is achieved by decreasing the working length and increasing the rotation speed of the parallel grooved metering device for wheat seeds. However, increasing the rotation speed of the metering device would be unpleasant to exploit small electric motors with a gearbox. As rotation speed increases, the rotation torque decreases proportionately. A helical-grooved metering device is preferred to ensure the even distribution of granular fertilizers or wheat seeds at full working length^[25,26]. However, when the active roller length is reduced to 15-30 mm, the workflow is identical to that of a parallel-grooved metering device at a low speed^[27]. The parallel-grooved and helical-grooved metering devices with twelve grooves are used to discharge granular fertilizers and wheat seeds^[28]. It should be noted that more metering devices discharge granular fertilizers than wheat seeds. High doses of granular fertilizers and wheat seeds are 600 kg/hm² and 125 kg/hm², respectively.

Rollers with six grooves have an extensive working volume and are capable of metering high doses of granular fertilizers at a low rotation speed, but the uniform distribution of the granular fertilizer is achieved only at a high rotation speed with a reduced working length^[3,29-33]. High doses of fertilizers are dispensed by a belt-type metering device^[34,35]. However, the design of the belt-type metering device is intricate. A spirally grooved metering device^[36-39] and studded feed roller^[40,41] significantly improve uniform granular fertilizer distribution at slow rotation speeds. However, the spiral-grooved dispenser is sensitive when used in hilly terrain. As the slope changes, the discharged dose of particles increases or decreases. It must be considered that granular fertilizer absorbs moisture from the air due to its hygroscopic nature^[42,43]. In case, when granular fertilizer seeders apply wet granular fertilizers due to improper storage, the fertilizer gets trapped in passive zones located on the front side of the stud^[34,44]. To prevent passive zone, a new design of a pin-roller is proposed, where the pins are in the form of a truncated pyramid eliminating the passive zones. It is considered that determining the position of the pins on the pin-roller allows for the even application of a high dose of fertilizers and wheat seeds at low rotation speeds.

The tube effect is also investigated as the granular fertilizers and wheat seeds' even distribution may depend on tube type and inclination. Experiments with corn and rapeseed show that the tube design affects the collision frequency and distribution uniformity^[45-47]. The seeders are recommended not to use the tubes in the metering device^[48]. However, in many conventional seeders with hoppers, the particles are moved from the hopper to the colters by gravity. The particle leaving the metering device is accelerated by gravity, but the frictional characteristics of the particle in the tube influence the particle speed. The particle shape and tube conditions (new or worn) or the tube inclination and length affects the particle discharge^[49-51]. This can lead to gaps in the particle row or blockage of the feed tube^[52-54]. As long as a new pin-roller metering device is designed, it is imperative to investigate the final distribution of granular fertilizers and wheat seeds influenced by tubes into the soil.

According to the over mentioned issues, there are three objectives of this research. First and foremost, determining the optimum position of the pins in the form of a truncated pyramid to provide an even distribution of high doses of granular fertilizers and wheat seeds based on contrary responses, such as the Slip Rate (SR) of the particles between the pins and the coefficient of variation (CV) of discharged particles. Second, comparing the optimized pin-roller configuration with the commonly used six-grooved and twelve-grooved rollers. The frame of the six-grooved, twelve-

grooved, and pin-roller metering devices are interchangeable and convenient for providing experiments by changing the rollers. The last is investigating the tube type and inclination influence when the pin-roller, six-grooved, and twelve-grooved rollers are used. The final particle discharge when the particles are applied into the soil is essential, and the investigation of the tube effect is also used to compare the metering devices.

2 Materials and methods

2.1 Analysis of pin-roller parameters

The granular fertilizer or wheat seed volume flow rate V_k , was considered as the dependent variable and was defined as the ratio of the weight flow rate Q_k to the bulk density ρ . The volume of fertilizer flow per revolution of the pin roller is equal to the following:

$$V_k = V_b + V_a \quad (1)$$

where, V_b is the working volume of the pin-roller, mm³; V_a is the volume of the active layer, mm³.

The working volume of the pin roller is equal to:

$$V_b = V_e - V_i - V_p \quad (2)$$

where, V_e is the volume of the pin-roller based on the outer radius r_1 , mm³; V_i is the volume of the cylinder based on the inner radius r_2 , mm³; V_p is the volume of the pins, mm³ (Figure 1).

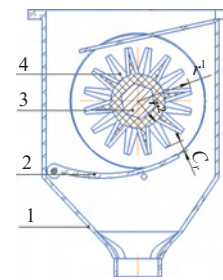


Figure 1 Metering device

The pins are in a line, and the number of pins in the lines is the same, but there is another pin in the adjacent line; two pins located at the edges make up half and count as one (Figure 2).

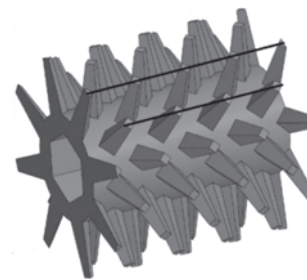


Figure 2 Pin-roller metering device

$$V_e = \pi(r_2 + h)^2 * L \quad (3)$$

where, r_1 is the outer radius of the pin-roller, $r_1 = (r_2 + h)$, mm; L is the length of the pin-roller, mm; h is the height of the pin, mm (Figure 3).

$$V_i = \pi \cdot r_2^2 \cdot L \quad (4)$$

The shape of the pin is a truncated pyramid, and the bottom and top of the pyramid are square. Therefore

$$V_p = k \left(\frac{1}{3} h (c^2 + cb + b^2) \right) \quad (5)$$

where, k is the number of pins on the roller surface; c is the square

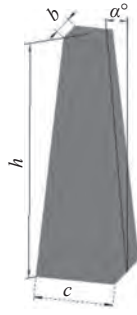


Figure 3 Parameters of the roller pin

side length of the bottom, mm; b is the length of the top square side, mm; h is the pin's height, mm.

Moreover, it also has to be mentioned that the length of the top square side (b) is a variable parameter depending on the pin inclination angle (α). Therefore,

$$V_p = k \left(\frac{1}{3} h \left(c^2 + c \left(c - 2h \cdot \text{tg} \alpha^\circ \right) + \left(c - 2h \cdot \text{tg} \alpha^\circ \right)^2 \right) \right) \quad (6)$$

$$V_a = \left[\pi(r_2 + h + c_r)^2 - \pi(r_2 + h)^2 \right] \cdot L \quad (7)$$

where, $c_r=1-3$ mm, the thickness of the active layer.

When the pin-roller is rotating, the particles between the pins can slip relative to the pin, as the particles between the pins interact with the particles on the active layer. The slippage rate also depends on the particle shape, friction properties of the materials and particles, the thickness of the active layer, pin quantity, and shape. A lot of factors influence the particle slippage rate. Therefore, the SR is determined as follows:

$$\text{SR} = \left(1 - \frac{Q_{(\text{exp})}}{Q_{(k)}} \right) \times 100\% \quad (8)$$

where, $Q_{(\text{exp})}$ is the experimentally determined weight flow rate per revolution; $Q_{(k)} = V_{(k)} \cdot \rho$.

The SR depends on the particle slippage between the pins. To optimize the parameters of the pin-roller metering device, SR should be zero or minimized as much as possible. Nevertheless, the slippage of particles between the pins is allowed rather than being broken or damaged.

At a given application rate, particles for one revolution of the drive wheel of the seeder should be sown:

$$Q_{1k} = \pi D_{dw} b_a z_{sd} Q \frac{1}{10^4} \quad (9)$$

where, Q is the given application rate, kg/hm²; D_{dw} is the diameter of the drive wheel, m; b_a is the width of the aisle, m; z_{sd} is the number of seeding devices. However, considering the density of the particles and the slip of the drive wheel, one device must seed the number of particles:

$$V_a = \frac{\pi D_{dw} b_a Q}{10^4 (1 - \varepsilon) \rho} \quad (10)$$

where, ε is the slip ratio of the drive wheel, $\varepsilon = 0.03 - 0.1$; ρ is the particle density, kg/m³.

The working volume of the reel will be:

$$V_k = \frac{\pi D_{dw} b_a Q}{10^4 (1 - \varepsilon) \rho i} \quad (11)$$

where, $i = \frac{n_{sa}}{n_{dw}}$ is the transmit ratio between the drive wheel and the reels; n_{sa} is the number of revolutions per minute of the reel; n_{dw} is the number of revolutions per minute of the drive wheel.

The expressions (3), (4), (6), (7), and (11) can be equated:

$$\begin{aligned} & \pi(r_2 + h)^2 \cdot L - \frac{3\sqrt{3}}{2} r_2^2 \cdot L - \\ & k \left(\frac{1}{3} h \left(c^2 + c \left(c - 2h \cdot \text{tg} \alpha^\circ \right) + \left(c - 2h \cdot \text{tg} \alpha^\circ \right)^2 \right) \right) + \\ & \left[\pi(r_2 + h + c_r)^2 - \pi(r_2 + h)^2 \right] \cdot L = \\ & \frac{\pi D_{dw} b_a Q}{10^4 (1 - \varepsilon) \rho i} \end{aligned} \quad (12)$$

Equation (12) connects all major structural and technological parameters. The design parameters include the pin rollers radius, the number of pins on it, and the height and dimensions of the lower bases, the diameter of the drive wheel. Technological parameters are as follows: the application rate, the width of the aisle, and transmit ratio. From the expression the seeding fertilizer in one revolution of the pin-roller by weight can be obtained:

$$Q_k = \frac{\pi D_{dw} b_a Q}{10^4 (1 - \varepsilon) i} \quad (13)$$

where, $i = \frac{n_{sa}}{n_{dw}}$, $n_{sa} = \frac{30w}{\pi}$, $n_{dw} = \frac{60v_m}{\pi D_{dw}}$.

Substituting these values into Equation (13), $Q_{(k)}$ is determined as follows:

$$Q_k = \frac{2\pi b_a Q v_m}{10^4 (1 - \varepsilon) w} \quad (14)$$

where, v_m is the traveling speed of the machine, m/s, w is the angular velocity of the pin-roller, rad/s.

From Equation (14), the value of the angular velocity of the pin-roller can be obtained:

$$w = \frac{2\pi b_a Q v_m}{10^4 (1 - \varepsilon) Q_k} \quad (15)$$

Knowing the angular velocity of the pin-roller and the given application rate, the electric motor speed can be controlled depending on the machine or tractor speed.

2.2 Determining the metering device parameters to simulate and compare on DEM

In this simulation experiment on DEM, the value ranges of the pin-roller parameters were as follows: the height of the roller pin (h) was 4-15 mm; the pin inclination angle (α) was 5°; the side length of the square bottom of the pin (c) was 5 mm. The new pin roller is based on the design of existing rollers, and compared to them, the length of the pin roller (L) and the outer radius of the pin roller (r_1) in all metering devices were 60 mm. The design of the experimental algorithms and the analysis were conducted in the Design-Expert 8.0.6 software, and the following three parameters, pin quantity in line, pin height, and pin lines, were marked as A, B, and C, respectively, and considered as factors. The pin-rollers are designed in 3D CAD software.

In the first stage of the simulation experiment on DEM, we have provided experiments with granular fertilizers and wheat seeds, according to the Central Composite Plan (CCP) algorithm with two factors and five levels (Table 1). The height of the pin was constant and equal to 15 mm.

Table 1 Codes of the CCP algorithm experimental factors

Code	(A) Pin quantity	(C) Pin lines
-2	3	8
-1	4	10
0	5	12
1	6	14
2	7	16

In the second stage of the simulation experiment on DEM, we have provided experiments only with wheat seeds according to the Box-Behnken algorithm with three factors and three levels (Table 2). In the second stage of the experiment, the target was to determine the interaction of wheat seeds with the metering device when the pin's height was considered a factor. The applying dose of the granular fertilizer (i.e., 600 kg/hm²) is more than the wheat seeds (i.e., 125 kg/hm²). The decrease in the height of the pin would decrease the discharged granular fertilizer dose. However, as long as the research purpose is to equip the metering device with a little electric motor, there was no need to provide experiments using granular fertilizers.

Table 2 Codes of the Box-Behnken algorithm experimental factors

Code	(A) Pin quantity	(B) Pin height/mm	(C) Pin lines
-1	3	4	14
0	4	7	16
1	5	10	18

The main parameters of the six and twelve-grooved rollers are demonstrated in Figure 4. The roller with twelve grooves is used to discharge wheat seeds and granular fertilizers, while the roller with six grooves is used to discharge only granular fertilizers. These two metering devices are compared with the pin-roller metering device with the optimized pin positions.

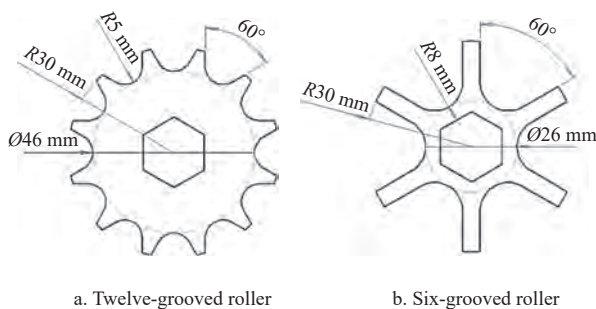


Figure 4 Main parameters of the rollers

2.3 Analysis of the particle behavior in the tube

Metering devices are rotating moving particles from the hopper to the tube. It takes some time for the particles to reach the ground. This period depends on tube type and tube position. When the particles pass a vertical pipe without any obstruction, the particles acquire an impact velocity when they reach the ground (Equation (16)).

$$\vartheta = \sqrt{2gH} \quad (16)$$

where, ϑ is the particle impact velocity with the ground, m/s; g is the acceleration due to gravity (9.81 m/s²); H is the vertical height of the metering device from the ground, mm.

The velocity obtained by the metering device is neglected independently of the rotation speed of the metering device as the particle's direction is changed by gravity. Therefore, when a particle is dropped from the metering device, the initial velocity is zero, and the total energy equals the potential energy (W_0) expressed in Equation (17).

$$W_0 = mgH \quad (17)$$

where, m is the weight of the particle, g.

When particles pass through a non-vertical tube, the particle speed is significantly reduced by the friction between the tube and

the particle. In this case, the particle acceleration (a) is expressed in Equation (18) (Figure 5).

$$\varepsilon = g \sin \beta - \mu g \cos \beta = g(\sin \beta - \mu \cos \beta) \quad (18)$$

where, a is the acceleration of a particle when it meets an obstacle, m/s²; μ is the coefficient of kinetic friction between the tube and the particle; β is the inclination of the tube, (°);

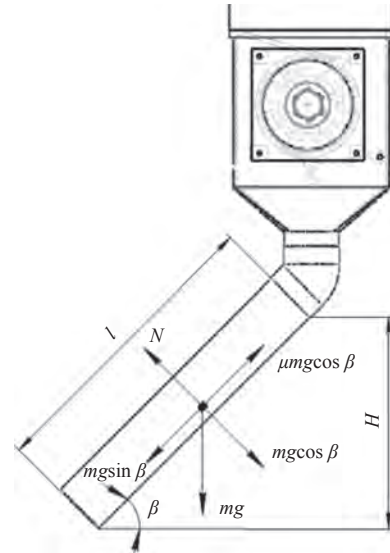


Figure 5 Parameters of the inclined tube and sliding particle direction forces in the case of smooth tube

The total acceleration force F of the particle is expressed in Equation (19).

$$F = ma = mg(\sin \beta - \mu \cos \beta) \quad (19)$$

The particle velocity when the tube is inclined is expressed in Equation (20)

$$v^2 = 2al = 2a \frac{H}{\sin \beta} = 2gH(1 - \mu \cos \beta) \quad (20)$$

where, l is tube length, mm.

The kinetic energy W_1 at the end of the tube is expressed in Equation (21).

$$W_1 = mgh(1 - \mu \cos \beta) \quad (21)$$

Equation (21) is fair when the particle is sliding; otherwise is not acceptable because of the collision between particle and tube that causes changes in the direction and velocity of the particle. The shape of the particle and tube type and dimensions significantly influence the particle behavior in the tube. If the particles are not spherical, the prediction of the particle behavior is complex. Therefore to evaluate particle behavior in the tube, the granular fertilizer and wheat seed particles are simulated in DEM software.

The next step was to determine the influence of the various tubes on the uniformity of particle distribution. Two factorial experiments were provided varying the length of tubes (l) and the angle of inclination (β). Smoothed and helical tubes are chosen to compare, as they are frequently used in seeders. The smoothed tube is cylindrical with an inner diameter of 30 mm. The dimensions and shape of the helical tube are shown in Figure 6.

The RSM was used to design the experiment. A factorial experiment with two factors varying the tube's length (l) and angle of inclination (β) was generated using Design-Expert software (Table 3). When determining the maximum angle, awareness should be taken the particles would not stop along the tube. Here, it must

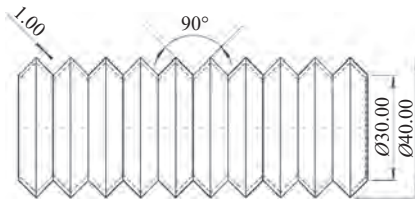


Figure 6 Dimensions of the helical tube

Table 3 Codes of the two factorial experiments

	Minimum level	Maximum level
Angle/(°)	15	45
Tube length/mm	200	1000

be mentioned that tube types and particle varieties are independent factors. Therefore, separated simulation experiments with granular fertilizer and wheat seeds should be provided according to two factorial experiment designs.

2.4 DEM input parameters

The discrete element method (DEM) was first developed by Cundall and Strack^[55-58] and is a numerical technique for simulating the mechanical behavior of granular assemblies. It has the advantage of data tracking, such as the trajectories, velocities, and transient forces of all particles at any test stage. This study uses calibrated input parameters from other research to simulate granular fertilizers and wheat seeds in DEM. The calibrated values of the material properties used in the Hertz-Mindlin no-slip numerical model for the DEM simulations were obtained from the literature (Table 4). The boundary conditions were not specified since it is out of research interest how the particles behave when leaving the domain. The Hertz-Mindlin no-slip model is well explained in the literature [59], and in this research, the Euler was selected as a time integration method. The Raleigh time-step was 30%. The estimated cell radius of the simulator grid was 3 mm. The inter-particle and particle-material interaction property values are shown in Table 5. The sphericity and size distribution of granular fertilizers were investigated, and the calibrated particle sizes on DEM were demonstrated in the literature [60]. The particles formed on DEM granular fertilizer are 100% spherical, while the sphericity of wheat seed particles is 60% (Figure 8)^[61]. The moisture content of granular fertilizers and wheat seeds was 2% and 14%, respectively. Studies at different humidity levels were not carried out due to the lack of interaction properties of granular fertilizers and wheat seeds with additional moisture content calibrated by DEM. It should be noted that granular fertilizers at 4% moisture dramatically change physical and mechanical properties and are not allowed to use.

Table 4 Mechanical properties of the materials

Intrinsic parameters	Shear Modulus/Pa	Poisson's ratio	Density/kg·m ⁻³
Granular fertilizer	1.24×10 ⁷ (a)	0.25 (a)	1575 (a)
Wheat	1.13×10 ⁷ (b)	0.22 (b)	1370 (b)
Acrylic	1.15×10 ⁹ (c)	0.35 (c)	1385 (c)
PLA	2.42×10 ⁸ (d)	0.36 (d)	1050 (d)

Note: (a) [30]; (b) [62]; (c) [63]; (d) [64].

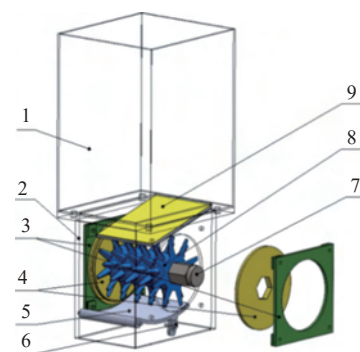
2.5 Experimental test rig to simulate particles on DEM and responses to evaluate the metering devices

First of all, to optimize the pins' position, an experimental setup without a bottom is used (Figure 7). The hopper (1) is connected to the top of the metering device frame with bolts (2), and the left and right outer caps (3) are attached to the left and right sides of the metering device frame with screws. The screws keep the left and right inner caps (4) adjacent to the dispenser body with

Table 5 Interparticle and particle-material interaction property values

Interaction properties	Coefficient	Related investigations
Fertilizer-fertilizer rolling friction coefficient	0.05	
Fertilizer-fertilizer static friction coefficient	0.30	
Fertilizer-fertilizer coefficient of restitution	0.58	
Fertilizer-acrylic rolling friction coefficient	0.08	
Fertilizer-acrylic static friction coefficient	0.266	[60]
Fertilizer-acrylic coefficient of restitution	0.531	
Fertilizer-PLA rolling friction coefficient	0.099	
Fertilizer-PLA static friction coefficient	0.294	
Fertilizer-PLA coefficient of restitution	0.491	
Wheat-wheat rolling friction coefficient	0.36	
Wheat-wheat static friction coefficient	0.15	
Wheat-wheat coefficient of restitution	0.25	
Wheat-acrylic rolling friction coefficient	0.29	
Wheat-acrylic static friction coefficient	0.36	[61]
Wheat-acrylic coefficient of restitution	0.79	
Wheat-PLA rolling friction coefficient	0.35	
Wheat-PLA static friction coefficient	0.30	
Wheat-PLA coefficient of restitution	0.5	

the possibility of rotation around its axis. The inner caps (4) have a hexagonal hole in the center. The lower flap (5) is located in the lower part of the metering device frame (2) and is connected to the metering device frame with a cotter pin on one side and a bolt on the other. Since the bolt adjusts the position of the lower flap by softening and tightening, it is called the bolt adjuster (6). The center of the hexagonal roller shaft (7) and pin-roller (8) is aligned with the center of the inner caps and rotated counterclockwise with them. On the upper side of the metering device frame, there is an inclined top flap (9) that guides the particles moving under the action of gravity. The simulations on EDEM were provided with various pins' positions to optimize. The hopper (1), metering device frame (2), and inclined top flap (9) are made of acrylic material, while others are directly interacting with granular fertilizers, and wheat seeds are made of PLA material.



1. Hopper 2. Metering device frame 3. Left and right outer caps 4. Left and right inner caps 5. Lower flap 6. Bolt adjuster 7. Hexagonal roller shaft 8. Pin-roller 9. Inclined top flap

Figure 7 Test rig to optimize pin-roller parameters

The pin-roller with optimized pins' positions is compared with other rollers on an experimental test rig without a bottom (Figure 8a). The experimental test rig with a bottom is used to study the effect of the bottom (Figure 8b) before investigating the impact of tubes on the particle discharge process (Figure 8c). Two types of tubes with different angles and lengths are attached to the bottom of the metering device.

The working process of the experiment is described step by step using a test rig with a helical tube (Figure 9). A 1:1 scale 3D CAD drawing of the dispenser is created and saved as a ".STEP" file, which is then imported into the EDEM software (Figure 9a). Then, three-particle collection boxes are created at the bottom of the test rig, and three square particle factories are inside the bottom of the hopper. A particle factory is a virtual plane that generates particles at an initial speed (Figure 9b). In total, 10 000 particles were generated in each hopper at an initial speed of 0.1 m/s in two seconds (Figure 9c). The resulting particles first fill the free space and then the hopper. After two seconds, the roller begins to rotate at a speed of 10 r/min, and the particles filling the free space of the rollers move along with the rollers until they pass the lower flap and fall (Figure 9d). The fallen

particles are collected in a box (Figure 9e). It should be noted that to apply a high dose of granular fertilizers and wheat seeds, 5 r/min would be enough. Nevertheless, to get more discharged particles during the discharge, the rotation speed was chosen as 10 r/min. The total simulation time was approximately 16 s with 2 s for the generation of particles in the hopper. The monitoring zones of 50 mm³ were created, covering the box to measure the particle flow mass (Figure 9f). The particle mass was recorded every 0.05 s during the period of 6-16 s, giving a total of 200 readings. The data was saved in an Excell file and analyzed. In this research, granular fertilizers and wheat seeds are described as a particle. Granular fertilizers are used to demonstrate the working principle. However, the movement of the granular fertilizers is shown by vector.

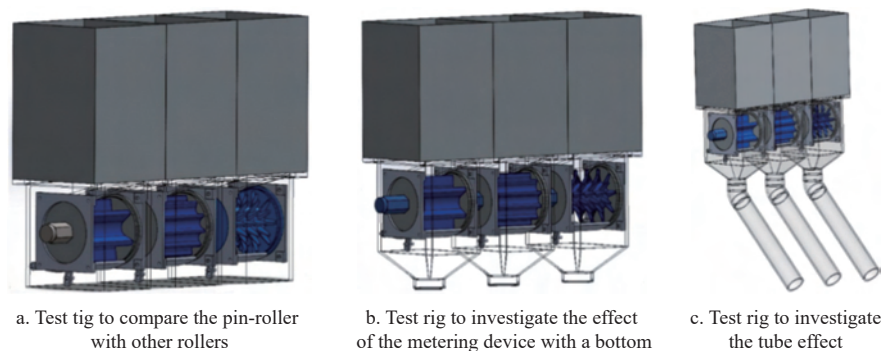


Figure 8 Experimental test rigs

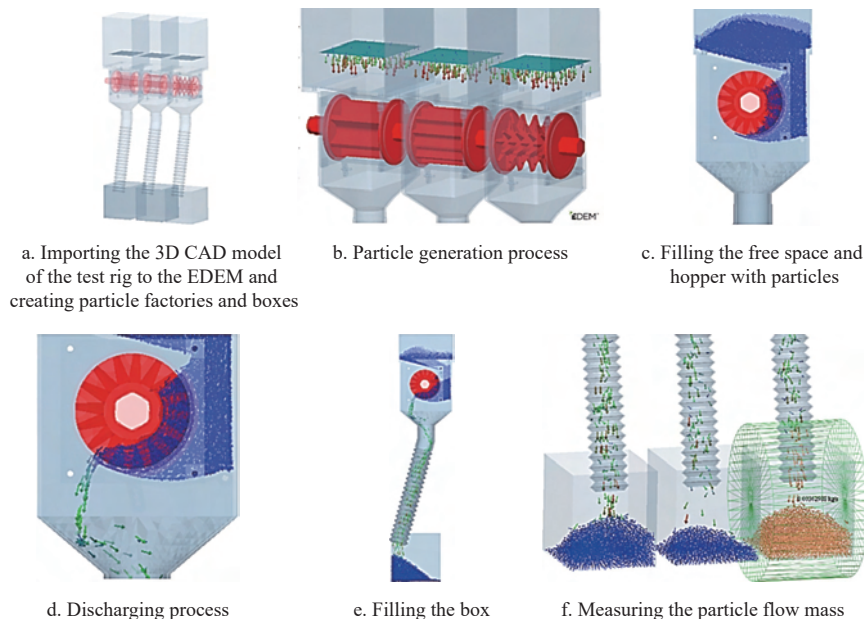


Figure 9 Simulation process

The CV is a leading response to evaluating the performance of metering devices^[11,13,23,30,49-50]. As the particles slip between the pins, the SR of particles is chosen as a second indicator to evaluate the performance of the pin-roller. The particle slippage between the pins is not efficiently using the working volume of the metering device. Therefore, SR should be minimized as well as CV. The particle quantity (Q) discharged within 60 s of the metering devices is chosen as a third indicator to evaluate the performance of a metering device. However, the particle quantity (Q) discharged within 60 s of the metering devices depends on the SR of the particles between the pins.

After determining the optimum pins' positions, a new pin-roller

is compared with six and twelve-grooved metering devices. It is fair enough to compare the pin-roller metering devices with existing ones using the same method. Comparison of the pin roller with other rollers and the influence of different types of tubes and their position is estimated by the CV value.

3 Results and discussion

3.1 Analysis of the first stage simulation experiment results

The simulation experiments on DEM were provided in identical conditions with granular fertilizers and wheat seeds. When providing experiments with granular fertilizers and wheat seeds, the thickness of the active layer (c_r) was 1 mm. The results of the first

stage simulation experiments are shown in Table 6. As the pin's height was 15 mm, the $Q_{(exp)}$ of the pin-roller metering devices was more than the roller with six grooves. Therefore, further, the results of the $Q_{(exp)}$ are not analyzed, as any parameter of the pin-roller satisfies our target.

Statistical analysis was performed on the output values of the CV of granular fertilizer and wheat seeds and SR of granular

fertilizer and wheat seeds at a rotational speed of the pin-roller of 10 r/min (Tables 7 and 8). All the models are strongly significant. *A* and *B* both factors strongly influence the CV of granular fertilizer and wheat seeds, while the *B* factor has a negligible effect on the SR of granular fertilizer and wheat seeds compared with the *A* factor. Equations (22)-(25), in terms of coded factors, identify the relative impact of the factors and make predictions of each significant factor.

Table 6 Results of the first stage simulation experiment on DEM with a comparison of 12-grooved and 6-grooved rollers

№	(A) Pin quantity	(B) Pin lines	Granular fertilizer				Wheat seeds			
			$Q_{(k)}/g$	$Q_{(exp)}/g$	$SR_{(fer)}/\%$	$CV_{(fer)}/\%$	$Q_{(k)}/g$	$Q_{(exp)}/g$	$SR_{(wh)}/\%$	$CV_{(wh)}/\%$
1	4	10	142.98	1247.45	12.75	44.45	107.55	1012.05	5.90	48.48
2	6	10	138.08	1262.85	8.55	82.12	103.87	1034.45	0.41	82.17
3	4	14	139.06	1264.05	9.10	39.74	104.60	996.65	4.72	43.05
4	6	14	132.21	1183.65	10.47	75.49	99.45	956.25	3.85	82.91
5	3	12	143.96	1199.65	16.67	30.67	108.28	1011.65	6.57	33.94
6	7	12	132.21	1208.25	8.61	90.79	99.45	992.45	0.21	95.22
7	5	8	142.98	1267.25	11.37	61.41	107.55	1030.85	4.15	64.94
8	5	16	133.19	1206.45	9.42	54.47	100.19	989.85	1.20	57.16
9	5	12	138.08	1261.65	8.63	62.91	103.87	1017.05	2.08	67.45
10	5	12	138.08	1263.85	8.47	62.88	103.87	1017.65	2.02	66.24
11	5	12	138.08	1265.45	8.36	62.19	103.87	1016.65	2.12	65.11
12	5	12	138.08	1264.05	8.46	61.41	103.87	1013.45	2.43	65.30
13	5	12	138.08	1265.65	8.34	59.40	103.87	1018.05	1.99	68.32
12-grooved			788.65		80.74		635.25		96.07	
6-grooved			1183.85		111.13					

Table 7 ANOVA on the output values of the CV of granular fertilizer and wheat seeds to the various pin positions

Source	df	Sum of Squares	$CV_{(fer)}$			$CV_{(wh)}$			
			Mean Square	<i>F</i> -value	<i>p</i> -value	Sum of Squares	Mean Square	<i>F</i> -value	<i>p</i> -value
Model	5	3199	639.9	108.8	<0.0001	3292.1	658.4	131.71	<0.0001
A	1	3125	3124	531.2	<0.0001	3205.4	3205	641.2	<0.0001
B	1	52.93	52.93	9	0.02	34.18	34.18	6.84	0.0347
AB	1	0.92	0.92	0.16	0.7045	9.53	9.53	1.91	0.2099
A2	1	1.54	1.54	0.26	0.6251	5.38	5.38	1.08	0.3339
B2	1	20.95	20.95	3.56	0.1011	42.76	42.76	8.55	0.0222
Residual	7	41.18	5.88			34.99	5		
Lack of Fit	3	32.72	10.91	5.16	0.0734	27.35	9.12	4.77	0.0826
Pure Error	4	8.46	2.11			7.64	1.91		
Cor Total	12	3240				3327.1			
$R^2=0.9873$; Adj $R^2=0.9782$; Pred $R^2=0.8934$; Adeq precision=39.173; $CV=4\%$; $R^2=0.9895$; Adj $R^2=0.982$; Pred $R^2=0.9136$; Adeq precision=43039; $CV=3.46\%$.									

Note: * shows that the item is significant ($p < 0.05$); ** shows that the item is extremely significant ($p < 0.01$).

Table 8 ANOVA on the output values of the CV of granular fertilizer and wheat seeds to the various pin positions

Source	df	Sum of Squares	$SR_{(fer)}$			$SR_{(wh)}$			
			Mean Square	<i>F</i> -value	<i>p</i> -value	Sum of Squares	Mean Square	<i>F</i> -value	<i>p</i> -value
Model	5	66.52	13.3	19.61	0.0005	39.52	7.9	6.73	0.0133
A	1	29.91	29.91	44.08	0.0003	30.42	30.42	25.9	0.0014
B	1	2.63	2.63	3.88	0.0896	1.1	1.1	0.94	0.3646
AB	1	7.78	7.78	11.46	0.0117	5.33	5.33	4.53	0.0707
A2	1	25.3	25.3	37.29	0.0005	2.58	2.58	2.19	0.1823
B2	1	5.49	5.49	8.09	0.0249	0.56	0.56	0.48	0.5124
Residual	7	4.75	0.68			8.22	1.17		
Lack of Fit	3	4.7	1.57	116	0.0002	8.1	2.7	87.4	0.0004
Pure Error	4	0.054	0.013			0.12	0.031		
Cor Total	12	71.27				47.74			
$R^2=0.9334$; Adj $R^2=0.8858$; Pred $R^2=0.335$; Adeq precision=14.877; $CV=8.29\%$; $R^2=0.8277$; Adj $R^2=0.7047$; Pred $R^2=-0.4798$; Adeq precision=8.795; $CV=37.44\%$.									

Note: * shows that the item is significant ($p < 0.05$); ** shows that the item is extremely significant ($p < 0.01$).

$$CV(fer) = 61.73 + 16.14A - 2.1B \tag{22}$$

$$CV(wh) = 66.35 + 16.34A - 1.69B - 1.37B^2 \tag{23}$$

$$SR(fer) = 8.52 - 1.58A + 1.39AB + 1.05A^2 + 0.48B^2 \tag{24}$$

$$SR(wh) = 2.44 - 1.59A \tag{25}$$

From Equations (22)-(25), it is mentioned that *A* and *B* are contrary to each other to minimize the CV and SR. Decreasing the *A* factor and increasing the *B* factor decreases the CV but increases the SR and vice versa. The *AB* interaction is a significant factor for fertilizer SR and needs to be discussed (Figure 10). When *A* and *B* are close to their maximum and close to their minimum, the SR of fertilizer increases dramatically. When *A* and *B* are close to their maximum, the free space between the pins decreases dramatically, increasing the likelihood of particles getting trapped between them. Particles trapped between the pins will rotate with the pin-roller, disrupting the working process and not efficiently using the free space of the pin-roller. When *A* and *B* are close to their minimum, the free space between the pins gets large, and due to insufficient interaction with pins, the SR of granular fertilizers increases.

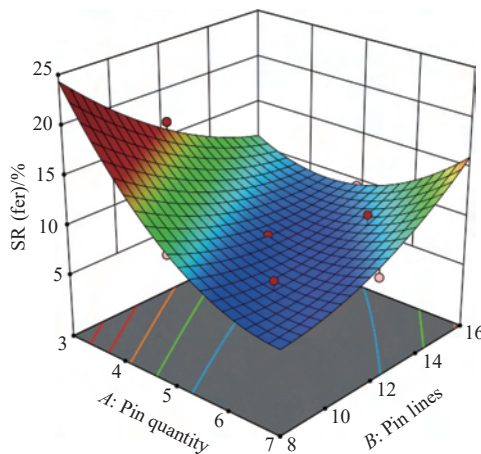


Figure 10 Response surface of the SR(fer) versus the AB interaction.

The optimized parameters of the pin-roller taken by Design-

Expert software show that the results are identical for granular fertilizer and wheat seeds. When the CV and SR of granular fertilizer and wheat seeds are strived to be a minimum *A*=4 and *B*=16, and *CV*_(fer), *CV*_(wh), *SR*_(fer), and *SR*_(wh) are 38%, 37%, 8%, and 2%, respectively. The CVs of the granular fertilizers and wheat seeds were similar, while the SR of the granular fertilizers was higher than the wheat seeds. It is considered due to the shape of the particles.

3.2 Analysis of the second stage simulation experiment results

The second stage of the simulation experiment on DEM has been provided with wheat seeds. The results of the second stage simulation experiments on DEM, according to the Box-Behnken algorithm, are shown in Table 9.

Table 9 Results of the second stage simulation experiments on DEM according to the Box-Behnken algorithm

Std Order	(A) Pin quantity	(B) Pin height	(C) Pin lines	<i>Q</i> _{(k)/g}	<i>Q</i> _{(exp)/g}	CV/%	SR/%
1	3	4	16	59.23	495.02	40.83	16.43
2	5	4	16	57.66	553.77	47.65	3.96
3	3	10	16	105.56	937.51	37.03	11.19
4	5	10	16	101.63	950.17	71.43	6.51
5	3	7	14	84.38	741.64	38.44	12.10
6	5	7	14	81.97	787.78	63.36	3.90
7	3	7	18	83.35	749.00	36.14	10.14
8	5	7	18	80.26	743.74	52.01	7.33
9	4	4	14	58.84	521.31	42.32	11.40
10	4	10	14	104.58	967.64	49.54	7.47
11	4	4	18	58.06	552.51	40.56	4.83
12	4	10	18	102.61	954.06	42.47	7.02
13	4	7	16	82.49	768.18	47.27	6.87
14	4	7	16	82.49	771.41	45.39	6.48
15	4	7	16	82.49	771.52	45.28	6.47

According to the Box-Behnken algorithm, the ANOVA of pin-roller parameters to the results of the experiment shows the significance of the models as well as factors and interaction between factors (Table 10). *A* factor has a strong influence on all the responses, while the *B* factor has a strong effect on CV and *Q*. *C* factor has a substantial impact on the CV.

Table 10 ANOVA of pin-roller parameters to the results of the simulation experiment on DEM according to the Box-Behnken algorithm

Source	df	CV/%				SR/%				<i>Q</i> /g			
		Sum of Squares	Mean Square	<i>F</i> -value	<i>p</i> -value	Sum of Squares	Mean Square	<i>F</i> -value	<i>p</i> -value	Sum of Squares	Mean Square	<i>F</i> -value	<i>p</i> -value
Model	9	1294.1	143.79	39.38	0.0004	152.99	17	6.11	0.0302	3.61e+05	40147.98	399	<0.0001
A	1	840.86	840.86	230.31	<0.0001	99.1	99.1	35.63	0.0019	1576.3	1576.3	15.68	0.0107
B	1	105.89	105.89	29	0.003	2.47	2.47	0.8864	0.3897	3.56e+05	3.56e+05	3538	<0.0001
C	1	63.12	63.12	17.29	0.0088	3.86	3.86	1.39	0.2917	45.44	45.44	0.452	0.5312
AB	1	190.08	190.08	52.06	0.0008	15.16	15.16	5.45	0.0668	531.07	531.07	5.28	0.0699
AC	1	20.44	20.44	5.6	0.0643	7.29	7.29	2.62	0.1663	660.54	660.54	6.57	0.0504
BC	1	7.03	7.03	1.93	0.2238	9.38	9.38	3.37	0.1257	501.49	501.49	4.99	0.0758
A ²	1	49.86	49.86	13.66	0.0141	11.95	11.95	4.3	0.0929	808.38	808.38	8.04	0.0364
B ²	1	0.0286	0.0286	0.0078	0.9329	4.59	4.59	1.65	0.2552	1699.95	1699.95	16.91	0.0092
C ²	1	12.42	12.42	3.4	0.1244	0.0061	0.0061	0.0022	0.9644	0.0045	0.0045	0	0.9949
Residual	5	18.25	3.65			13.91	2.78			502.58	100.52		
Lack of fit	3	17.66	5.89	19.93	0.0481	13.8	4.6	87.11	0.0114	495.39	165.13	45.95	0.0214
Pure error	2	0.5908	0.2954			0.1056	0.0528			7.19	3.59		
Cor total	14	1312.36				166.9				3.62e+05			
		<i>R</i> ² =0.9873; Adj <i>R</i> ² =0.9782; Pred <i>R</i> ² =0.8934; Adeq precision=39.173; CV=4%.				<i>R</i> ² =0.9895; Adj <i>R</i> ² =0.982; Pred <i>R</i> ² =0.9136; Adeq precision=43039; CV=3.46%.				<i>R</i> ² =0.9334; Adj <i>R</i> ² =0.8858; Pred <i>R</i> ² =0.3353; Adeq precision=14.877; CV=8.29%.			

Note: * shows that the item is significant (*p* < 0.05); ** shows that the item is extremely significant (*p* < 0.01).

Equations (26)-(28) in terms of coded factors are used to make predictions about the response for given levels of each significant factor. The coded equations identify the relative impact of the essential factors by comparing the factor coefficients.

$$CV = 45.65 + 10.25A + 3.64B - 2.81C + 6.89AB + 3.67 \quad (26)$$

$$SR = 6.61 - 3.52A \quad (27)$$

$$Q = 770.37 + 14.04A + 210.85B - 14.8A^2 - 21.46B^2 \quad (28)$$

C factor has little effect on the CV, and the impact on Q and SR is insignificant and eliminated. The increase of the C factor decreases CV. The B factor is the most influencing factor on Q, while the A factor has a superb effect on the CV. A is a single factor that influences the SR. The more pin quantities inline, the less SR (Equation 27). However, the more pin quantities in line, the more CV that is undesirable (Figure 11). When there are a lot of pins in line, the working process of the pin-roller will be close to the existing rollers. While optimizing the parameters, the SR is taken as a second necessary response as the slippage of particles between the pins is allowed to prevent particle damage. The CV is the most critical response in optimizing the parameters of the pin-roller. In the second stage of the experiment, our target is to investigate the interaction of wheat seeds with the pin roller. Therefore, Q was not included as a response as it significantly depends on pin height. The optimization results of Design-Expert Software were A=4, B=9 mm, and C=18, minimizing CV and SR by 35% and 8%. It is assumed that pin lines increased because the diameter of the pin-roller was more than in the previous experiment. The second stage experiments show that decreasing the pin's height does not give substantial improvements at the same valve speed. Therefore, the results of the first stage experiment are recommended to discharge granular fertilizers and wheat seeds.

3.3 Comparison results of metering devices with a bottom and without in DEM.

The comparison result of the different metering devices with a bottom and without a bottom is given in Figure 12. The smaller the CV, the more evenly the dosing device distributes the particles. As can be seen from the figure, the bottom of the metering device positively influences the uniformity of the particle discharge as the CVs are relatively lower. The pin-roller distributed the particles more uniformly without the bottom and with the bottom compared with other rollers. The twelve-grooved roller distributes particles more evenly than the six-grooved roller.

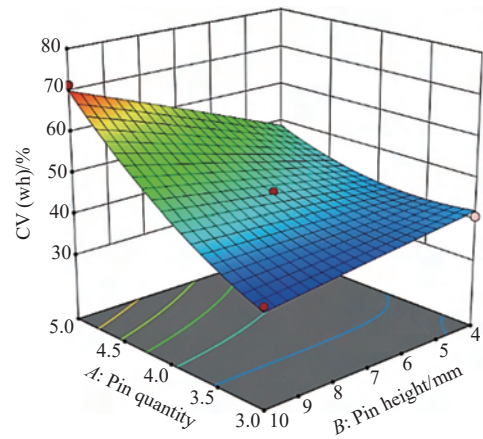


Figure 11 Interaction of the A and B factors affects the CV

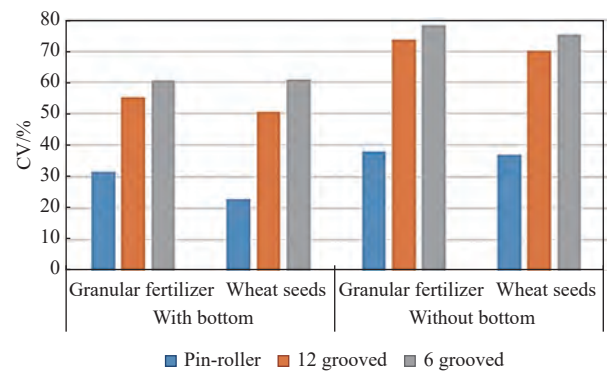


Figure 12 Comparison result of the metering devices with a bottom and without

3.4 Two factorial simulation experiment results with different tubes in DEM

The simulation results of the metering devices with smoothed and helical tubes are provided according to the factorial experiment with granular fertilizer, wheat seeds, and various metering devices are shown in Figure 13. The CV was the primary response to compare. The lower the CV, the better the even distribution of particles. The CV of the pin-roller is the lowest and does not exceed 30% at any angle of inclination and length of a smooth tube for granular fertilizer and wheat seed. The CVs of the twelve-grooved and the six-grooved rollers are getting lower when the helical tube is used than the smoothed tube when the tube inclination angle is increased from 15° to 45° as for granular fertilizer particles and

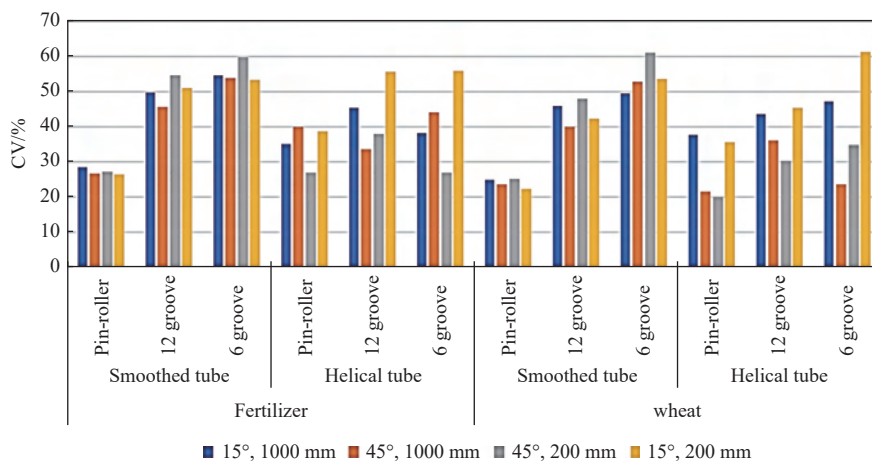


Figure 13 Two factorial experiment results with granular fertilizer and wheat seeds

wheat seeds.

The CVs of metering devices with the bottom and the CV of those with various tubes are subtracted to show the tube parameters effect (Figure 14). The positive data shows that using the tube implies the improvement of the uniformity of the discharged particles and vice versa. For the pin-roller metering device, the smooth tube's influence is positive when fertilizer particles are discharged, but when wheat seeds are discharged, the influence is little but negative. Therefore, using the smooth tube is recommended for the pin-roller, as the helical tube comparatively increases the CVs. When metering devices with twelve and six grooves are used, the smooth tube's influence is negligible, but the

influence of the helical tube is positive. When considering the length of the tube, the longer the tube, the more time it needs to pass the tube, which is undesirable. The time depends on the type of tube and the tube inclination angle. Twelve-grooved and six-grooved metering devices are recommended with the helical tube as the even distribution is improved. However, it is not feasible to determine the optimal length and angle of inclination of the helical tube to improve the even distribution of the particles due to the chaotic behavior of particles (Figure 15). Moreover, determining the optimal parameters and position of the helical tube for twelve-grooved and six-grooved metering devices was not the research concern.

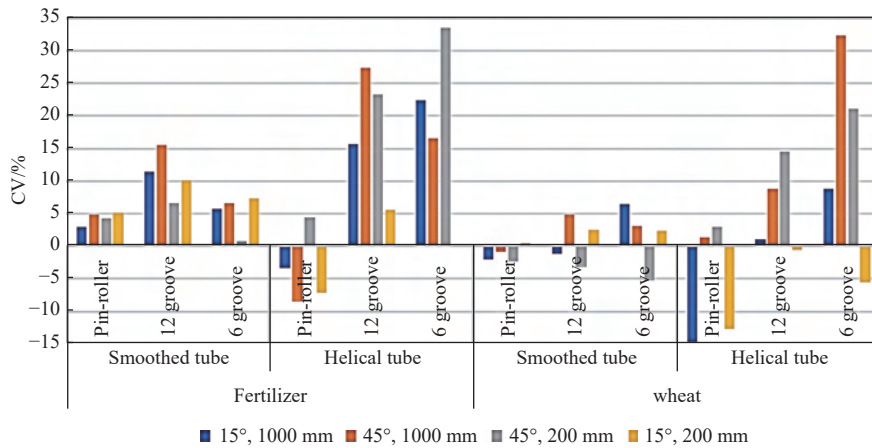


Figure 14 Results of adjusting the CVs of metering devices with a bottom and CVs of metering devices with different tubes

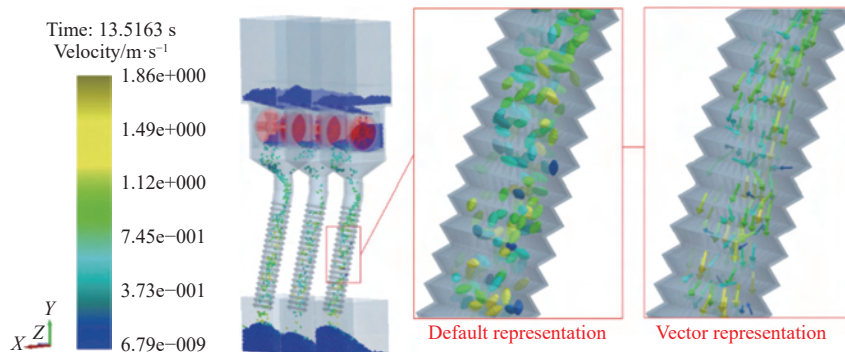


Figure 15 Chaotic behavior of wheat seeds in the helical tube

3.5 Study of particle shape influence

Data from two factorial experiments were organized to calculate the Pearson correlation coefficient (Table 11). To determine how much the shape of granular fertilizer and wheat seed influences when various tubes are used, the Pearson correlation coefficient was determined for smoothed and helical tubes according to their inclination angle and length using the Origin Pro software (Table 12). The CV data for granular fertilizers are selected as one data set, while wheat seed CV is chosen as a second data set using the same tube. According to the result, the correlation coefficients of the smoothed tube are close to one, meaning that the difference between the granular fertilizer and wheat seed shape has little influence on the discharge uniformity. Nevertheless, the helical tube's correlation coefficients are far from one or zero, meaning the difference between the granular fertilizer and wheat seed shape has a weak and less significant influence on the discharge uniformity depending on tube inclinations and the length.

Table 11 Results of two factorial experiments on calculating the Pearson correlation coefficient describe the influence of the particle shape

$\beta/(\circ)$	l/mm	Device	Smoothed tube		Helical tube	
			$CV_{(fer)}/\%$	$CV_{(wh)}/\%$	$CV_{(fer)}/\%$	$CV_{(wh)}/\%$
15	1000	Pin-roller	28.62	24.95	34.89	37.62
		12-grooved	49.63	45.81	45.38	43.57
		6-grooved	54.74	49.42	38.11	47.07
45	1000	Pin-roller	26.70	23.70	40.02	21.57
		12-grooved	45.53	39.87	33.80	35.94
		6-grooved	53.93	52.70	43.92	23.51
45	200	Pin-roller	27.21	25.21	27.08	19.95
		12-grooved	54.57	47.91	37.91	30.22
		6-grooved	59.77	61.15	27.01	34.81
15	200	Pin-roller	26.44	22.42	38.63	35.61
		12-grooved	51.05	42.19	55.52	45.21
		6-grooved	53.22	53.54	55.839	61.34

Table 12 Pearson correlation coefficient describing particle shape influences for smoothed and helical tubes

$\beta/(\circ)$	l/mm	Smoothed tube	Helical tube
15	1000	0.998	0.437
45	1000	0.988	0.869
45	200	0.975	0.210
15	200	0.956	0.794

4 Conclusions

Pin positions of the pin-roller have been determined to discharge a high dose of granular fertilizers and wheat seeds, minimizing the CV and SR. According to the analysis, it is determined that CV and SR are contrary response indicators. The simulation experiment's first stage results determined the optimal pin positions: the number of pins in a line is four, and the number of lines is sixteen. However, the lines can be decreased or increased depending on the pin-roller diameter. The optimized pin-roller is compared with six-grooved and twelve-grooved rollers at low rotation speeds. When the rollers with six and twelve grooves rotate at 10 r/min, the CV of the granular fertilizer distribution is 111.13% and 80.74%, respectively, and the CV of the wheat seed distribution is 96%. However, the CV of granular fertilizers and wheat seeds does not exceed 37% when a new pin-roller is rotating at 10 r/min. The CV of existing metering devices can be reduced by increasing the valve speed and reducing the working length. However, our goal was to lower the valve speed so that small electric motors could drive metering devices in a precision farming system. Thus, the calibrated pin-roller parameters allow the metering devices to discharge large doses of granular fertilizers and wheat seeds uniformly at low valve speeds. Moreover, we have investigated the impact of the particles' shape as granular fertilizer and wheat seeds on the particle discharge when smooth or helical tubes are used. As a result, we have determined the following:

- 1) The uniformity of the pin-roller metering device is low and can be used without tubes;
- 2) The pin-roller metering device is better to use with a smooth tube rather than a helical tube as the impact of the helical tube is negative;
- 3) Twelve-grooved or six-grooved rollers can be used with both tubes, but we recommend using a helical tube tilted a few degrees more to prevent excessive particle collision with the tube and more minor than to avoid tube clogging.

Acknowledgements

The authors appreciate the financial support provided by the National Key Research and Development Program of China (Grant No. 2018YFD0701102).

[References]

- [1] Cisternas I, Velásquez I, Caro A, Rodríguez A. Systematic literature review of implementations of precision agriculture. *Computers and Electronics in Agriculture*, 2020; 176: 105626.
- [2] Dobermann A, Blackmore S, Cook S E, Adamchuk V I. Precision farming: challenges and future directions. in Proceedings of the 4th International Crop Science Congress. Brisbane, Australia, 2004; Oct.26: 217p.
- [3] Sandoval J, Eugenio R, Cruz I, Canteñs G. Mechatronic system for the control of fertilizer and pesticide granules dispensers of a fertilizer seeder. *Revista Mexicana de Ciencias Agrícolas*, 2018; 21: 4355–4369.
- [4] Yu H F, Ding Y Q, Liu H T, Zhu W Q, Liu G Q, Fu X Q, et al. Optimization design and application of variable rate fertilization system for small-scaled fields. *Transactions of the CSAE*, 2018; 34(3): 35–41. (in Chinese)
- [5] Yu H F, Ding Y Q, Fu X Q, Liu H T, Jin M F, Yang C L, et al. A solid fertilizer and seed application rate measuring system for a seed-fertilizer drill machine. *Computers and Electronics in Agriculture*, 2019; 162: 836–844.
- [6] Cancan S, Zhou Z Y, Zang Y, Zhao L Q, Yang W W, Luo X W, et al. Variable-rate control system for UAV-based granular fertilizer spreader. *Computers and Electronics in Agriculture*, 2020; 180: 105832.
- [7] Song C C, Zhou Z Y, Jiang R, Luo X W, He X G, Ming R. Design and parameter optimization of pneumatic rice sowing device for unmanned aerial vehicle. *Transactions of the CSAE*, 2018; 34(6): 80–88. (in Chinese)
- [8] Su D X, Yao W X, Fenghua Y, Liu Y H, Zheng Z Y, Wang Y L, et al. Single-neuron PID UAV variable fertilizer application control system based on a weighted coefficient learning correction. *Agriculture*, 2022; 12(7): 1–22.
- [9] Li L, Qian L, Yan-yan C. Half-precision self-walking variable fertilization seeder design. *International Journal of Hybrid Information Technology*, 2016; 9(6): 177–188.
- [10] Yang S, Wang X, Zhai C Y, Dou H J, Gao Y Y, Zhao C J. Design and test on variable rate fertilization system supporting seeding and fertilizing monitoring. *Transactions of the CSAM*, 2018; 49(10): 145–153. (in Chinese)
- [11] Nukeshev S, Eskhozhin K, Eskhozhin D, Syzdykov D. Justification of design and parameters of seeding unit for fertilizers. *Journal of the Brazilian Society of Mechanical Sciences and Engineering*, 2017; 39(4): 1139–1149.
- [12] Brown E. Sowing seeds for the agricultural revolution: Jethro Tull (1674–1741). *Tractor*, 2003.
- [13] Jin, M F, Ding Y Q, Yu H F, Liu H T, Jiang Y Z, Fu X Q. Optimal structure design and performance tests of seed metering device with fluted rollers for precision wheat seeding machine. *IFAC Paperonline*, 2018; 51(17): 509–514.
- [14] Beaujot N, Vennard G, Markham N. Air seeder tank and distribution apparatus. *Seedmaster Manufacturing Ltd*, 2017.
- [15] Ess D R, Hawkins S E, Young J C, Christmas E P. Evaluation of the performance of a belt metering system for soybeans planted with a grain drill. *Applied Engineering in Agriculture*, 2005; 21(6): 965–969.
- [16] Tishkov N M, Makhonin V L, Nosov V V. Soybean seed yield and yield quality depending on the fertilizers doses and application methods. *Oil Crops*, 2019; 180: 53–60.
- [17] Gao J, Zhang J X, Zhang F, Hou Z Y, Zhai Y H, Ge L Z. Analysis of movement law and influencing factors of hill-drop fertilizer based on SPH algorithm. *Applied Sciences*, 2020; 10(9): 1643–1653.
- [18] Beard T, Maaz T, Borrelli K, Harsh J, Pan W. Nitrogen affects wheat and canola silica accumulation, soil silica forms, and crusting. *Journal of Environmental Quality*, 2018; 47(6): 1380–1388.
- [19] Gollany H T, Allmaras R R, Copeland S M, Albrecht S L, Douglas C L. Tillage and nitrogen fertilizer influence on carbon and soluble silica relations in a Pacific Northwest mollisol. *Soil Science Society of America Journal*, 2005; 69(4): 1102–1109.
- [20] Wiggerhauser M, Bigalke M, Imseing M, Keller A, Rehkemper M, Wilcke W. Using isotopes to trace freshly applied cadmium through mineral phosphorus fertilization in soil-fertilizer-plant systems. *Science of the Total Environment*, 2019; 648: 779–786.
- [21] Colaco A F, Molin J P. Variable rate fertilization in citrus: a long term study. *Precision Agriculture*, 2017; 18(2): 169–191.
- [22] Li X Z, Hao M D, Zhao J, Wang Z, Fu W, Liu Z Z. Effect of long-term fertilization on wheat yield under different precipitation patterns. *Chinese Journal of Applied Ecology*, 2018; 29(10): 3237–3244.
- [23] Antonangelo J A, Firmano R, Alleoni L, Oliveira A, Zhang H L. Soybean production under continuous potassium fertilization in a long-term no-till oxisol. *Agronomy Journal*, 2019; 111(5): 2462–2472.
- [24] Nukeshev S, Eskhozhin K, Karaivanov D, Sankibaev T, Kakabayev N. Theoretical and experimental substantiation of the design of an opener for intrasoil broadcast sowing of grain crops. *Bulgarian Journal of Agricultural Science*, 2016; 22(5): 862–868.
- [25] Gurjar B, Sahoo P K, Kumar A. Design and development of variable rate metering system for fertilizer application. *Journal of Agricultural Engineering Research*, 2018; 54(3): 12–21.
- [26] Nukeshev S, Yeskhozhin K, Tokusheva M, Zhazykbayeva Z. Substantiation of the parameters of the central distributor for mineral fertilizers. *International Journal of Environmental and Science Education*,

- 2016; 11: 7932–7945.
- [27] Kara M, Bayhan A K, Ozsert I, Yildirim Y. Performance of fluted roll metering devices in seed drills with ammonium sulphate and diammonium phosphate. *Applied Engineering in Agriculture*, 2010; 26(2): 197–201.
- [28] Nukeshev S, Sugirbay A. Fertilizer metering apparatus. Eurasian Scientific Association, 2015; 1: 24-27. (in Russian)
- [29] Lv H, Yu J Q, Fu H. Simulation of the operation of a fertilizer spreader based on an outer groove wheel using a discrete element method. *Mathematical and Computer Modelling*, 2013; 58(3-4): 836–845.
- [30] Ding S P, Bai L, Yao Y X, Yue B, Fu Z L, Zheng Z Q. Discrete element modelling (DEM) of fertilizer dual-banding with adjustable rates. *Computers and Electronics in Agriculture*, 2018; 152: 32–39.
- [31] Lv H, Yu J Q, Fu H. Simulation of the operation of a fertilizer spreader based on an outer groove wheel using a discrete element method. *Mathematical and Computer Modelling*, 2013; 58(3-4): 836–845.
- [32] Zeng S, Tan Y P, Wang Y, Luo X W, Yao L M, Huang D P, et al. Structural design and parameter determination for fluted-roller fertilizer applicator. *Int J Agric & Biol Eng*, 2020; 13(2): 101–110.
- [33] Feng H M, Gao N N, Li Y, Fu W Q, Guo Y M. Control method for parameters coordinate match of fluted roller fertilizer apparatus. *INMATEH Agricultural Engineering*, 2020; 60(1): 211–220.
- [34] Eskhozhin D, Nukeshev S, Zhaksylykova Z, Eskhozhin K, Balabekova A. Design and study of a dispenser for the introduction of the main batch of mineral fertilizers. *Mechanika*, 2018; 24(3): 343–351.
- [35] Zhaksylykova Z, Eskhozhin D, Nukeshev S, Akhmetov Y, Yeskhozhin K. Design of the construction and parameters justification of stud-belt seeding machine for application of the main dose of mineral fertilizer. *International Journal of Environmental and Science Education*, 2016; 11: 12959–12972.
- [36] Maleki M R, Jafari J F, Raufat M H, Mouazen A M, De B J. Evaluation of seed distribution uniformity of a multi-flight auger as a grain drill metering device. *Biosystems Engineering*, 2006; 94(4): 535–543.
- [37] Zhang L P, Zhang L X, Zheng W Q. Fertilizer feeding mechanism and experimental study of a spiral grooved-wheel fertilizer feeder. *Journal of Engineering Science and Technology Review*, 2018; 11(2): 107–115.
- [38] Ovtov V A, Polikanov A V, Orekhov A A, Shumaev V V, Gudim V M. Theoretical studies of geometric and kinematic parameters of a roller transporting device. *Нива Поволжья*, 2020; 1(54): 13–17.
- [39] Nukeshev S O, Romanyuk N N, Yeskhozhin K J, Zhunusova A E. Methods and results of the research of the fertilizer distributor of cutter-ridger-fertilizer. *Herald of Science of S. Seifullin Kazakh Agro Technical University*, 2016; 3(90): 138–145.
- [40] Boydas M G, Turgu N. Effect of vibration, roller design, and seed rates on the seed flow evenness of a studded feed roller. *Applied Engineering in Agriculture*, 2007; 23(4): 413–418.
- [41] Svensson J E T. Effects of constructional and operational variables on the mean mass-flow of particulate using a studded roller feeder. *Journal of Agricultural Engineering Research*, 1994; 59(4): 221–230.
- [42] Turan J J, Findura P J, Djalovic I G, Sedlar A D, Bugarin R M, Janic T V. Influence of moisture content on the angle of repose of nitrogen fertilizers. *International Agrophysics*, 2011; 25(2): 201–204.
- [43] De D. Flow behaviour of chemical fertilizers as affected by their properties. *Journal of Agricultural Engineering Research*, 1989; 42(4): 235–249.
- [44] Nukeshev S, Eskhozhin D, Lichman G, Karaivanov D, Zolotuhin E, Syzdykov D. Theoretical substantiation of the design of a seeding device for differentiated intra soil application of mineral fertilizers. *Acta Universitatis Agriculturae et Silviculturae Mendelianae Brunensis*, 2016; 64(1): 115–122.
- [45] Yazgi A. Effect of seed tubes on corn planter performance. *Applied Engineering in Agriculture*, 2016; 32: 783–790.
- [46] Lei X L, Hu H J, Wu W C, Liu H N, Liu L Y, Yang W H. Seed motion characteristics and seeding performance of a centralised seed metering system for rapeseed investigated by DEM simulation and bench testing. *Biosystems Engineering*, 2021; 203: 22–33.
- [47] Nukeshev S, Eskhozhin D, Karaivanov D, Yeskhozhin K. Determination of parameters of the main distributor for fertilizer applying machine. *Bulgarian Journal of Agricultural Science*, 2014; 20: 1513–1521.
- [48] Xi X B, Gu C J, Shi Y J, Zhao Y, Zhang Y F, Zhang Q. Design and experiment of no-tube seeder for wheat sowing. *Soil and Tillage Research*, 2020; 204: 104724.
- [49] Kocher M, Coleman J, Smith J, Kachman S. Corn seed spacing uniformity as affected by seed tube condition. *Applied Engineering in Agriculture*, 2011; 27(2): 177–183.
- [50] Yuan J, Liu Q, Liu X, Zhang T, Zhang X. Granular multi-flows fertilization process simulation and tube structure optimization in nutrient proportion of variable rate fertilization. *Transactions of the CSAM*, 2014; 45: 81–87. (in Chinese)
- [51] Lei X L, Liao Y T, Zhang Q S, Wang L, Liao Q X. Numerical simulation of seed motion characteristics of distribution head for rapeseed and wheat. *Computers and Electronics in Agriculture*, 2018; 150(10): 98–109.
- [52] Enderud H C. Influence of tube configuration on seed delivery to a coulter. *Journal of Agricultural Engineering Research*, 1999; 74(2): 177–184.
- [53] Alekseev E, Maksimov I, Terentev G, Maksimov E. Seed distribution by the coulter for the subsoil broadcast seeding. *Journal of Physics:Conference Series*, 2020; 1515: 042040.
- [54] Lain S, Sommerfeld M. Particle transport in turbulent flows along horizontal ducts. *Latin American Applied Research*, 2011; 41(5): 301–304.
- [55] Jafari M, Hemmat A, Sadeghi M. Comparison of coefficient of variation with non-uniformity coefficient in evaluation of grain drills. *Journal of Agricultural Science and Technology*, 2011; 13(5): 643–654.
- [56] Kim Y J, Kim H J, Ryu K H, Rhee J Y. Fertiliser application performance of a variable-rate pneumatic granular applicator for rice production. *Biosystems Engineering*, 2008; 100(4): 498–510.
- [57] Guler I E. Effects of flute diameter, fluted roll length, and speed on alfalfa seed flow. *Applied Engineering in Agriculture*, 2005; 21(1): 5–7.
- [58] Cundall P A, Strack O D. A discrete numerical model for granular assemblies. *Geotech*, 1979; 29(1): 47–65.
- [59] Li X Y, Du Y X, Liu L, Mao E R, Yang F, Wu J, et al. Research on the constitutive model of low-damage corn threshing based on DEM. *Computers and Electronics in Agriculture*, 2022; 194: 106722.
- [60] Adilet S, Zhao J, Sayakhat N, Chen J, Nikolay Z, Bu L X, et al. Calibration strategy to determine the interaction properties of fertilizer particles using two laboratory tests and DEM. *Agriculture*, 2021; 11(7): 592.
- [61] Sugirbay A, Hu G R, Chen J, Mustafin Z, Muratkhan M, Iskakov R, et al. A study on the calibration of wheat seed interaction properties based on the discrete element method. *Agriculture*, 2022; 12(9): 1497.
- [62] Horabik J, Wiącek J, Parafiniuk P, Bańda M, Kobyłka R, Stasiak M, et al. Calibration of discrete-element-method model parameters of bulk wheat for storage. *Biosystems Engineering*, 2020; 200(16): 298–314.
- [63] Marigo M, Stitt E H. Discrete element method (DEM) for industrial applications: comments on calibration and validation for the modelling of cylindrical pellets. *KONA Powder and Particle Journal*, 2015; 32(2): 236–252.
- [64] Moysey P A, Thompson M R. Determining the collision properties of semi-crystalline and amorphous thermoplastics for DEM simulations of solids transport in an extruder. *Chemical Engineering Science*, 2007; 62(14): 3699–3709.